DOI: 10.1002/ejic.201100241

Coordination Behavior and Coligand-Dependent *cis*/*trans* Isomerism of Calcium Bis(diphenylphosphanides)

Jens Langer,[a] Tareq M. A. Al-Shboul,[a] Fadi M. Younis,[a] Helmar Görls,[a] and Matthias Westerhausen*[a]

Keywords: Calcium / Strontium / Isomers / Phosphanides / Phosphinites

The salt metathesis reaction of $KPPh_2$ with CaI_2 and SrI_2 in THF yields the corresponding complexes $[(THF)_4Ae(PPh_2)_2]$ [Ae = Ca (**1**), Sr]. Depending on the crystallization conditions, *cis*- or *trans*-$[(THF)_4Ca(PPh_2)_2]$ can be isolated. In solution, a fast equilibrium converts these isomers into each other leading to a single set of resonances in the NMR spectra. The THF ligands can be replaced by stronger Lewis bases, such as *N*-methylimidazole (MeIm), which leads to the formation of $[(MeIm)_4Ae(PPh_2)_2]$ [Ae = Ca (**2a**), Sr (**2b**)]. The use of tetradentate hexamethyltriethylenetetramine (hmteta) fixes a *cis* configuration yielding [(hmteta)$Ca(PPh_2)_2$] (**3**). All compounds are very air and moisture sensitive, therefore a few crystals of the partially oxidized product [(hmteta)$Ca(PPh_2)(OPPh_2)$] (**4**) were also obtained.

Introduction

Calcium bis(phosphanides) are accessible through the metalation of phosphanes and metathetically by the reaction of potassium phosphanides with alkaline earth metal diiodides in THF.[1] THF is an ideal solvent because it is a strong base thus ensuring the solubility of calcium diiodide as $[(THF)_4CaI_2]$,[2,3] although the nearly quantitative precipitation of KI drives the metathesis reaction completely in favor of calcium bis(phosphanide). This metathetical approach gave pure $[(THF)_4Ca(PPh_2)_2]$,[4,5] which proved to be a valuable catalyst in hydrophosphanylation reactions of alkynes.[6,7] Nevertheless, with catalytic amounts of $[(THF)_4Ca(PPh_2)_2]$, reactions of $HPPh_2$ with substituted butadiynes gave various regio- and stereoisomers. The resulting C=C double bonds remained inactive during this procedure. In another reaction, heteroleptic calcium diphenylphosphanides showed catalytic hydrophosphanylation activity toward activated alkenes.[7,8] Due to the importance of calcium bis(diphenylphosphanide) in calcium-mediated hydro-phosphanylation reactions of alkynes, we were interested in varying the coordination sphere to tune the reactivity and regioselectivity of these catalysts.

Schleyer and co-workers[9] stated roughly 20 years ago that "the preferred anion orientation in unsolvated species will dominate the coordination geometries of the solvated complexes as well" because "anionic ligands are bound more strongly than neutral coligands" with bulky coligands leading to exceptions from this rule. Therefore, a *trans* arrangement of the phosphanide ligands in calcium bis(phosphanides) can be expected because this arrangement also minimizes electrostatic repulsion between the anions. This rule seems to be quite general because $[(THF)_4Ca(PPh_2)_2]$,[4,5] $[(THF)_4Ca\{P(H)Si\mathit{i}Pr_3\}_2]$,[10] and $[(THF)_4Ca\{P(SiMe_3)_2\}_2]$[11] crystallized with a *trans* arrangement whereas the bulky 1,3,5-trimethyl-1,3,5-triazinane ligand (tmta) enforces a bent P–Ca–P moiety with an angle of 110.2(1)° in $[(tmta)_2Ca\{P(SiMe_3)_2\}_2]$ and an octa-coordinate calcium atom.[12] Quantum chemical investigations on monomeric derivatives AeX_2 (X = CH_3, NH_2, OH, and F) show that linear molecules can be expected for the lighter alkaline earth metals, whereas strontium and barium tend to form bent molecules due to small but significant d-orbital contributions.[13] Calcium and especially the heavier homologous metals lie on the borderline between classic s-block elements and early transition metals with an increasing tendency to involve d-orbitals in bonding situations from calcium to barium. Recent calculations also showed dimethylcalcium to be bent.[14] Similar trends are valid for unsolvated halides[15] and hydrides[16] with CaF_2 being bent whereas the heavier halides show linear CaX_2 molecules in contrast to bent BaX_2. The solvation of CaI_2 (which shows a linear geometry if unsolvated) with mono-dentate Lewis bases L, such as ethers, yields $[(L)_4CaI_2]$ with a *transoid* arrangement of the iodide anions.[2,3,17] The addition of tetramethylethylenediamine [1,2-bis(dimethylamino)ethane, tmeda] leads to *trans*-$[(tmeda)_2CaI_2]$, however, tetradentate hexamethyltriethylenetetramine (hmteta) enforces a *cis* arrangement of the CaI_2 unit.[17] Additionally, the 1,2-dimethoxyethane adduct $[(dme)_2Ca(NPh_2)_2]$ adopts a *cis* arrangement.[18]

[a] Institute of Inorganic and Analytical Chemistry, Friedrich Schiller University,
Humboldtstrasse 8, 07743 Jena, Germany
Fax: +49-3641-948102
E-mail: m.we@uni-jena.de

Due to the importance of calcium bis(diphenylphosphanide) in catalytic hydrophosphanylation reactions we investigated the coordination behavior of this complex.

Results and Discussion

The metathesis reaction of $KPPh_2$ with CaI_2 in THF yields $[(THF)_4Ca(PPh_2)_2]$ (**1**),[4,5] which can be recrystallized after the removal of insoluble potassium iodide (Scheme 1). A careful investigation of the crystal shape showed two crystal morphologies, namely, cubic blocks and rod-shaped crystals. Therefore, crystallization conditions were investigated in more detail. At –40 °C, predominantly rod-shaped crystals of *cis*-$[(THF)_4Ca(PPh_2)_2]$ (*cis*-**1**) precipitated from concentrated solutions. After removal of this crystalline material the mother liquor was cooled and from this diluted solution orange-red blocks of *trans*-$[(THF)_4Ca(PPh_2)_2]$ (*trans*-**1**) predominantly formed. These findings were verified by X-ray structure determinations. Both isomers are shown in Scheme 2. In solution, only one set of signals can be observed by NMR spectroscopy. Upon cooling the solution, however, a shift of the singlet in the ^{31}P NMR spectra from δ = 13.1 (293 K) to δ = 18.0 ppm (203 K) was observed, accompanied by a slight broadening of the signal.

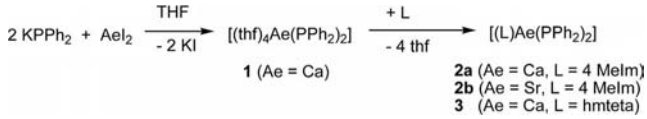

Scheme 1. Syntheses of **1**–**3**.

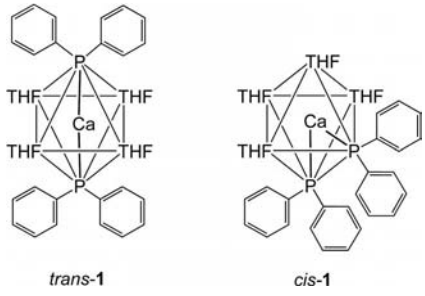

Scheme 2. Schematic drawing of *trans*-$[(THF)_4Ca(PPh_2)_2]$ (*trans*-**1**) and *cis*-$[(THF)_4Ca(PPh_2)_2]$ (*cis*-**1**), which precipitate depending on the crystallization conditions. Only the Ca–P bonds are drawn, the other lines represent the edges of the coordination octahedron.

The substitution of the coordinated THF molecules of $[(THF)_4Ca(PPh_2)_2]$ (**1**) with the stronger Lewis base *N*-methylimidazole (MeIm) was achieved by the addition of this azaligand to a THF solution of **1**. Recrystallization from a toluene/THF mixture gave orange-red single crystals of $[(MeIm)_4Ca(PPh_2)_2]$ (**2a**). A similar protocol gave orange-red crystals of the homologues strontium derivative $[(MeIm)_4Sr(PPh_2)_2]$ (**2b**). In both cases, the crystalline solids contained the *trans* isomers.

Due to the fact that the bis(tmeda) complex of calcium diiodide crystallized as a *trans* isomer and the hmteta adduct with a *cisoid* iodide arrangement, we substituted the THF ligands of **1** by hmteta. The major product was indeed the calcium complex $[(hmteta)Ca(PPh_2)_2]$ (**3**) with the diphenylphosphanide ligands in a *cisoid* fashion. There are two possible isomers with this structure (Scheme 3), namely, a complex with a *cis* or a *trans* configuration of the dimethylamino bases. Due to steric reasons, the *trans* isomer is formed. Traces of oxygen (from exposure to adventitious air) oxidized Ph_2P^- to $Ph_2P\text{-}O^-$ anions, which were also detected in solution by ^{31}P NMR spectroscopy. A very similar configuration was also observed for heteroanionic $[(hmteta)Ca(PPh_2)(OPPh_2)]$ (**4**), which was isolated together with the major product **3**.

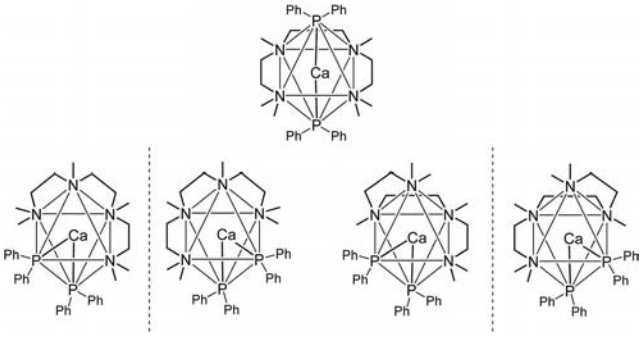

Scheme 3. Possible isomers for the hmteta complex **3** of calcium bis(diphenylphosphanide). The phosphorus atoms can be in a *trans* (top) or a *cis* arrangement with the dimethylamino groups in a *trans* (bottom, left) or *cis* orientation (bottom, right).

The initial objective of this investigation was the elucidation of the influence of a *cis* or *trans* arrangement of the diphenylphosphanides on the structural parameters and in a later study on the catalytic reactivity. From THF solutions, both isomers can be isolated depending on the crystallization conditions, however, an equilibrium, fast on the NMR time scale, leads to a single set of resonances in solution spectra. The molecular structure and numbering scheme of *cis*-**1** are represented in Figure 1.

Contrary to the expectation that *cis*-arranged bulky anions should enhance repulsive electrostatic and steric strain leading to enhanced bond lengths, the average Ca–P and Ca–O distances are smaller than observed for the *trans* isomer (Table 1). However, enhancement of the negative charge on the phosphorus atoms on replacement of the phenyl groups by trialkylsilyl substituents leads to smaller Ca–P distances as, for example, observed for $[(THF)_4Ca\{P(SiMe_3)_2\}_2]$ (av. Ca–P 291.8 pm[11]). In addition, smaller coordination numbers of calcium also lead to a contraction of the Ca–P bond[22] enhanced by incorporation of the phosphanide functionality in a bidentate ligand system.[22,23] Reduction of the charge on the phosphorus atom by delocalization, as in $[(THF)_3Ca\{(Me_2P)_2C\text{-}SiMe_3\}_2]$ {Ca–P ranging from 303.8(1) to 304.9(1) pm[24]}, or on the calcium atom by a covalently bound counter part, as in $[(THF)_4$-

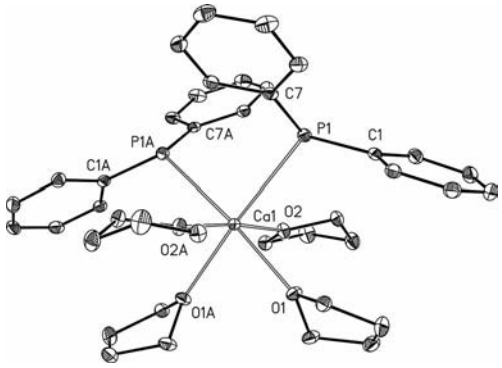

Figure 1. Molecular structure and numbering scheme of *cis*-[(THF)$_4$Ca(PPh$_2$)$_2$] (*cis*-**1**). The ellipsoids represent a probability of 40%, H atoms are omitted for clarity. Symmetry-related atoms (–*x*, *y*, –*z* + 1.5) are marked with the letter "A". Selected bond lengths [pm]: Ca1–O1 236.6(1), Ca1–O2 234.4(1), Ca1–P1 295.12(5), P1–C1 182.3(2), P1–C7 181.1(2); angles (deg.): P1–Ca1–P1A 95.55(2), P1–Ca1–O1 92.12(3), P1–Ca1–O2 93.41(3), P1–Ca1–O1A 170.29(3), P1–Ca1–O2A 90.43(3), O1–Ca1–O2 83.15(4), O1–Ca1–O1A 80.93(6), O1–Ca1–O2A 92.49(4), O2–Ca1–O2A 174.28(6), Ca1–P1–C1 117.18(5), Ca1–P1–C7 111.67(5), C1–P1–C7 106.69(7).

Ca(Ph)(PPh$_2$)] {Ca–P 301.0(2) pm[25]}, led to enlarged Ca–P distances. The phosphorus atoms in *cis*-**1** are in pyramidal environments and with this geometry, crowding is reduced by the diphenylphosphanide groups turning away from one another. The rather short Ca–O bonds and the fact that the Ca–O values *trans* to P and *trans* to O are similar, verify the lack of significant intramolecular strain.

Substitution of the THF ligands by *N*-methylimidazole leads to the alkaline earth metal complexes [(MeIm)$_4$Ae(PPh$_2$)$_2$] (**2a**: Ae = Ca; **2b**: Ae = Sr). The molecular structure and numbering scheme of **2a** is displayed in Figure 2, values for **2b** are given in the legend and listed in Table 1. The alkaline earth metal atoms are in distorted octahedral environments with *trans* arrangements of the diphenylphosphanyl ligands and form short bonds to the imidazole ligands leading to an elongation of the Ae–P bonds. The planar imidazole ligands represent strong Lewis bases with nearly planar coordinating N1 and N3 nitrogen atoms. These complexes show very similar molecular structures to those also observed for the corresponding *N*-methylimidazole adducts of ytterbium,[20] europium,[21] and samarium bis(diphenylphosphanide),[19] which are included for comparison in Table 1.

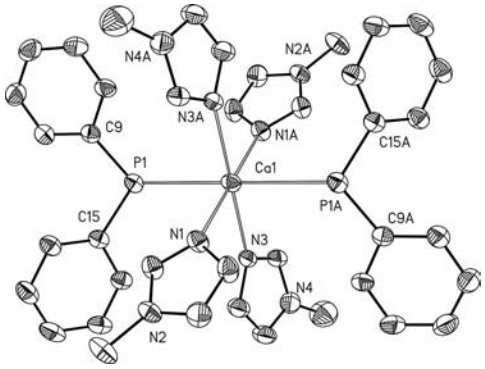

Figure 2. Molecular structure and numbering scheme of [(MeIm)$_4$Ca(PPh$_2$)$_2$] (**2a**). Ellipsoids represent a probability of 40%, H atoms are omitted for clarity. Symmetry-related atoms (–*x*, –*y*, –*z* + 1) are marked with the letter "A". Selected bond lengths of **2a** [of isotypic **2b** in square brackets] [pm]: Ae1–P1 303.8(1) [315.42(7)], Ae1–N1 245.2(3) [260.1(2)], Ae1–N3 244.1(3) [262.4(2)], P1–C9 181.0(4) [181.0(3)], P1–C15 181.5(4) [181.5(3)]; angles (deg.): P1–Ae1–P1A 180.0 [180.0], P1–Ae1–N1 91.72(8) [90.89(6)], P1–Ae1–N3 86.39(7) [91.66(5)], N1–Ae1–N3 85.35(10) [94.91(8)], Ae1–P1–C9 122.0(1) [111.67(9)], Ae1–P1–C15 115.2(1) [123.36(9)], C9–P1–C15 106.1(2) [107.0(1)].

The molecular structure and numbering scheme of [(hmteta)Ca(PPh$_2$)$_2$] (**3**) and [(hmteta)Ca(PPh$_2$)(OPPh$_2$)] (**4**) are represented in Figures 3 and 4, respectively. In both structures, the hmteta ligands show very similar conformations with the dimethylamino functionalities in a *trans* alignment. The Ca–N distances to the dimethylamino bases are smaller than those to the inner nitrogen atoms, which can be explained by an enhanced steric strain. This crowding also enhances the Ca–P bond lengths in comparison with those in the THF complex of calcium bis(diphenylphosphanide).[4,5] Furthermore, steric repulsion leads to increased angle sums of the phosphorus atoms as a consequence of the fact that the diphenylphosphanyl groups are straightened up toward the periphery of the complex.

Table 1. Average values of selected structural parameters of adducts of mononuclear calcium and strontium bis(diphenylphosphanide) of the type [(L)$_n$M(PPh$_2$)$_2$]. For comparison reasons [(THF)$_4$Ca(PPh$_2$)$_2$] (*trans*-**1**) as well as isotypic alkaline earth metal and lanthanoid complexes are included.

Compound	M–P	M–O/N	P–C	P–M–P	M–P–C	C–P–C	ΣP	Ref.
trans-[(THF)$_4$Ca(PPh$_2$)$_2$]	298.7	237.6	182.0	180	109.5/120.5	103.4	333.4	[4,5]
cis-[(THF)Ca(PPh$_2$)$_2$]	295.1	235.5	181.7	95.55	111.7/117.2	106.7	335.5	
trans-[(MeIm)$_4$Ca(PPh$_2$)$_2$]	303.8	244.7	181.3	180	115.2/122.0	106.1	343.3	
cis-[(hmteta)Ca(PPh$_2$)$_2$]	301.3	254.8	183.0	99.19	110.5/123.3	103.0	336.7	
trans-[(THF)$_4$Sr(PPh$_2$)$_2$]	314.3	252.1	181.8	177.4	101.6/106.2	107.3	316.6	[4,5]
trans-[(MeIm)$_4$Sr(PPh$_2$)$_2$]	315.4	261.3	181.3	180	111.7/123.4	107.0	342.1	
[(THF)$_5$Ba(PPh$_2$)$_2$]	333.7	274.7	181.6	157.1	105.6/115.7	106.0	327.2	[4]
[(18C6)Ba(PPh$_2$)$_2$]	334.8	278.5	181.9	160.8	97.9/101.8	105.3	306.0	[5]
trans-[(THF)$_4$Yb(PPh$_2$)$_2$]	299.1	243.4	184.3	180	110.2/119.4	103.1	332.7	[19]
trans-[(MeIm)$_4$Yb(PPh$_2$)$_2$]	302.8	249.1	181.4	180	114.6/123.0	106.4	343.9	[20]
trans-[(MeIm)$_4$Eu(PPh$_2$)$_2$]	312.7	260.8	181.5	180	113.7/123.0	106.6	343.3	[21]
trans-[(MeIm)$_4$Sm(PPh$_2$)$_2$]	313.9	262.1	180.8	180	112.8/124.3	106.3	343.1	[19]

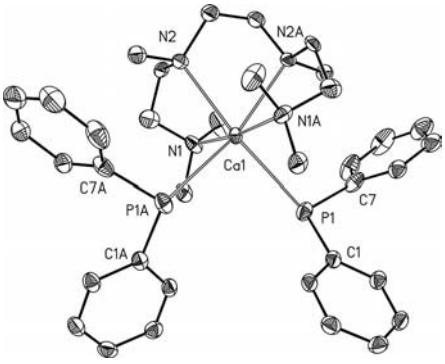

Figure 3. Molecular structure and numbering scheme of [(hmteta)-$Ca(PPh_2)_2$] (**3**). The ellipsoids represent a probability of 40%. H atoms are omitted for clarity. Symmetry-related atoms (*–x*, *y*, *–z* + 0.5) are marked with the letter "A". Selected bond lengths [pm]: Ca1–P1 301.3(1), Ca1–N1 251.5(3), Ca1–N2 258.0(6), P1–C1 181.8(4), P1–C7 184.2(4); angles (deg.): P1–Ca1–P1A 99.19(5), P1–Ca1–N1 88.56(8), P1–Ca1–N2 153.6(1), P1–Ca1–N1A 95.83(7), P1–Ca1–N2A 99.4(1), N1–Ca1–N2 71.0(1), N1–Ca1–N1A 173.2(2), N1–Ca1–N2A 103.2(1), N2–Ca1–N2A 70.4(2), Ca1–P1–C1 123.3(1), Ca1–P1–C7 110.5(1), C1–P1–C7 103.0(2).

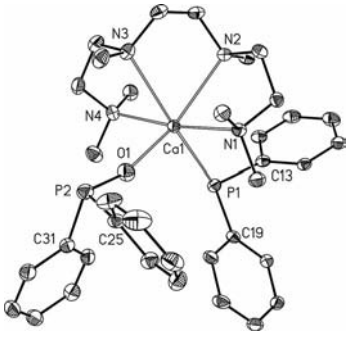

Figure 4. Molecular structure and numbering scheme of [(hmteta)-$Ca(PPh_2)(OPPh_2)$] (**4**). The ellipsoids represent a probability of 40%, H atoms are omitted for clarity. Selected bond lengths [pm]: Ca1–P1 302.0(1), Ca1–O1 216.7(3), Ca1–N1 252.0(4), Ca1–N2 262.1(4), Ca1–N3 263.8(4), Ca1–N4 258.3(4), P1–C13 182.9(5), P1–C19 182.8(4), O1–P2 155.6(3), P2–C25 184.2(5), P2–C31 185.2(5); angles (deg.): P1–Ca1–O1 103.0(1), P1–Ca1–N1 98.02(9), P1–Ca1–N2 101.58(9), P1–Ca1–N3 152.66(9), P1–Ca1–N4 87.3(1), O1–Ca1–N1 95.3(1), O1–Ca1–N2 153.5(1), O1–Ca1–N392.9(1), O1–Ca1–N4 88.0(1), N1–Ca1–N2 71.5(1), N1–Ca1–N3 102.5(1), N1–Ca1–N4 173.0(1), N2–Ca1–N3 68.8(1), N2–Ca1–N4 103.0(1), N3–Ca1–N4 71.0(1), Ca1–O1–P2 161.4(2), Ca1–P1–C13 110.6(1), Ca1–P1–C19 110.1(1), C13–P1–C19 103.1(2), O1–P2–C25 104.3(2), O1–P2–C31 103.8(2), C25–P2–C31 98.4(2).

In complex **4**, one of the phosphanyl groups is oxidized leading to the diphenylphosphinite anion $[Ph_2PO]^-$. In this anion the phosphorus atom is in a pyramidal environment with a small angle sum of 306.5°. The P–O bond length of 155.6(3) pm is very small. A larger value of 159.62(2) pm was observed for the bridging Ph_2PO^- anion with a three-coordinate oxygen atom between two calcium atoms in $[(bdi)Ca(\mu\text{-}OPPh_2)]_2$, in which bdi refers to the anion formed by deprotonation of 2-[(2,6-diisopropylphenyl)-amino]-4-[2,6-diisopropylphenylimino]pent-2-ene.[26] The Ca1–O1 bond length of 216.7(3) pm in complex **4** is very short due to a strong electrostatic attraction. The calcium alkoxides do not provide useful data for comparison because of their complex oligomeric structures.[27]

Conclusion

THF complexes of alkaline earth metal bis(diphenylphosphanides) can adopt *cis* and *trans* configurations, which are in a fast equilibrium in solution. Depending on the crystallization conditions, for example, the concentration of the mother liquor and crystallization temperature, *cis* or *trans* isomers can be crystallized. The coordination of tetradentate hexamethyltriethylenetetramine (hmteta) enforces a *cis* arrangement of the diphenylphosphanide ligands.

The angle sums of the phosphorus atoms reflect the steric hindrance between the phosphanide ligands and the neutral coligands (THF, MeIm, or hmteta). In no case is a planar coordination of the phosphorus atom observed. Stronger bases, such as *N*-methylimidazole, cause an elongation of the Ca–P bonds. These alkaline earth metal compounds form crystal structures that are similar to those of the ytterbium, europium, and samarium analogues, exemplifying an often-observed relationship. Future studies to clarify the influence of the configuration on the reactivity and catalytic behavior of these complexes will be facilitated by the isolation of compounds with well-defined *cis* and *trans* configurations.

Experimental Section

General: All manipulations were carried out in an argon atmosphere under anaerobic conditions. Prior to use, all solvents were thoroughly dried and distilled under an argon atmosphere. In many cases, it was not possible to weigh out a definite amount because the compounds were so sensitive to air and moisture that they decomposed, at least partially, during this procedure. Therefore, the analyses are limited to NMR spectroscopy and X-ray structure determinations. ^1H, $^{31}P\{^1H\}$, and ^{13}C NMR spectra were recorded in $[D_8]$THF solutions at ambient temperature on a Bruker AC 200 MHz or a Bruker AC 400 MHz spectrometer. All spectra were referenced to 98% perdeuterated THF as an internal standard. Starting $[(THF)_4Ae(PPh_2)_2]$ (Ae = Ca, Sr) was prepared metathetically according to a literature procedure[4,5] from $KPPh_2$ and AeI_2.

Isolation of *cis*-$[(THF)_4Ca(PPh_2)_2]$ (*cis*-1): A solution of $KPPh_2$ in THF (0.5 M, 9.7 mL, 4.85 mmol) was added to a solution of anhydrous CaI_2 (0.71 g, 2.42 mmol) in THF (40 mL). During this procedure, a colorless precipitate of KI formed and the solution turned orange-red. The reaction mixture was stirred an additional hour at room temperature and filtered to remove the solid. The mother liquor was reduced to approximately 20 mL by vacuum distillation and stored at –40 °C overnight. The formed orange-yellow rod-like crystals were collected on a cooled Schlenk frit and gently dried in vacuo. The crystals tended to lose cocrystallized THF upon prolonged drying. Yield: 0.69 g (0.82 mmol, 34%).

Crystals of this crop were identified as *cis*-**1**·2THF by X-ray diffraction experiments. From the mother liquor, orange-red blocks were obtained by prolonged storage at –40 °C, identified as the *trans* isomer (Note that the crystal shape is not sufficient to distinguish

between the isomers, as under differing conditions the *trans* isomer was obtained in the form of yellow needles).[5]

[(MeIm)$_4$Ca(PPh$_2$)$_2$] (2a). Method A: *N*-Methylimidazole (MeIm, 0.13 mL, 1.69 mmol) was added to an orange solution of [(THF)$_4$-Ca(PPh$_2$)$_2$] (295 mg, 0.42 mmol) in THF (15 mL) at room temperature. After 20 min all volatiles were removed in vacuo and the residue washed with hexane. Recrystallization from a mixture of toluene and THF (ratio 3:1) at –30 °C afforded red crystals of **2a** (0.23 g, 74%).

Method B: A solution of KPPh$_2$ in THF (0.5 M, 6.1 mL, 3.05 mmol) was added dropwise to a solution of anhydrous CaI$_2$ (455 mg, 1.55 mmol) in THF (10 mL). The reaction mixture turned orange. MeIm (0.51 mL) was then added dropwise to this reaction mixture. Filtration (removal of insoluble KI), removal of all volatiles, washing with hexane, and recrystallization from a mixture of benzene and THF (ratio 3:1) gave red crystals of **2a** (0.81 g, 71%). Complex **2a** is soluble in THF but insoluble in aliphatic and aromatic hydrocarbons.

M.p. 137–140 °C (dec.). (C$_{40}$H$_{44}$CaN$_8$P$_2$, 738.86): calcd. C 65.02, H 6.00, N 15.17; found C 64.82, H 6.12, N 14.93. ^{1}H NMR: δ = 3.60 (s, Me), 6.8–7.7 (Ph, Im) ppm. ^{13}C NMR: δ = 32.7 (s, Me), 120.2 (s, Im), 129.1 (s, Ph), 129.2 (d, J_{PC} = 6.2 Hz, Ph), 129.9 (s, Im), 134.6 (d, J_{PC} = 17.1 Hz, Ph), 138.4 (s, Im) ppm; *ipso*-C signal not visible. ^{31}P{^{1}H} NMR: δ = –13.6 (s) ppm. IR (Nujol): $\tilde{\nu}$ = 3109 (w), 3052 (m), 2951 (w), 1967 (w), 1897 (w), 1828 (w), 1673 (m), 1590 (m), 1518 (s), 1437 (s), 1285 (m), 1231 (w), 1201 (sh br), 1126 (w), 1063 (m), 1027 (m), 999 (w), 923 (m), 907 (m), 818 (m), 749 (s), 720 (vs), 698 (s), 663 (s), 617 (m), 565 (m), 539 (w) cm^{-1}.

[(MeIm)$_4$Sr(PPh$_2$)$_2$] (2b). Method A: *N*-Methylimidazole (0.11 mL, 1.34 mmol) was added at room temperature to an orange solution of [(THF)$_4$Sr(PPh$_2$)$_2$] (250 mg, 0.334 mmol) in THF (20 mL). After 30 min the solvent was removed in vacuo and the residue washed with toluene. Recrystallization at –30 °C from a mixture of toluene and THF (ratio 3:1) afforded **2b** (0.2 g, 77%).

Method B: Addition of a solution of KPPh$_2$ in THF (0.5 M, 3.3 mL, 1.63 mmol) to a solution of [(THF)$_5$SrI$_2$] (577 mg, 0.82 mmol) in THF (10 mL) caused an immediate color change to orange. The subsequent addition of MeIm (0.26 mL) deepened the orange color. Filtration and removal of all volatile materials left a residue that was washed with toluene and recrystallized from a mixture of toluene and THF (ratio 3:1). Cooling to –30 °C gave red crystalline **2b** (0.51 g, 80%). This compound is soluble in THF but insoluble in aliphatic and aromatic hydrocarbons.

M.p. 121–123 °C (dec.). (C$_{40}$H$_{44}$N$_8$P$_2$Sr, 786.40): calcd. C 61.09, H 5.64, N 14.25; found C 60.00, H 5.93, N 13.64. ^{1}H NMR: δ = 3.60 (s, Me), 6.4–7.0 and 7.3–7.6 (Ph, Im) ppm. ^{13}C NMR: δ = 33.0 (Me), 120.2 (br., Ph), 120.4 (Im), 127.7 (br., Ph), 129.8 (Im), 130.9 (br., Ph), 139.4 (Im) ppm; *ipso*-C not found. ^{31}P{^{1}H} NMR: δ = –6.8 (s) ppm. IR (Nujol): $\tilde{\nu}$ = 3111 (m), 3056 (m), 2993 (w), 2953 (w), 2917 (w), 2343 (w), 1965 (w), 1896 (w), 1822 (w), 1775 (w), 1631 (w), 1581 (m), 1517 (vs), 1475 (s), 1436 (s), 1421 (w), 1285 (s), 1231 (s), 1231 (s), 1191 (sh br), 1128 (w), 1079 (m), 1026 (m), 979 (w), 921 (m), 908 (m), 816 (s), 741 (s), 699 (s), 663 (s), 617 (s), 561 (m), 530 (m) cm^{-1}.

[(hmteta)Ca(PPh$_2$)$_2$] (3) and [(hmteta)Ca(PPh$_2$)(OPPh$_2$)] (4): Hexamethyltriethylenetetramine (0.38 g, 1.65 mmol) was added to a stirred suspension of *trans*-[(THF)$_4$Ca(PPh$_2$)$_2$] (1.048 g, 1.50 mmol) in toluene (15 mL). The resulting reaction mixture was stirred for 2 h at room temperature. The yellow precipitate of **3** was collected on a Schlenk frit and dried in vacuo. The mother liquor was stored at –40 °C for several days resulting in the formation of a few tiny yellow platelets of **4**·1.5toluene. Yield: 0.94 g (1.47 mmol, 98%) of yellow **3**. Characterization of **3**: ^{1}H NMR: δ = 2.15 (s, 12 H, Me), 2.20 (s, 6 H, Me), 2.37 (m, 4 H, CH$_2$), 2.42 (s, 4 H, CH$_2$), 6.61 (br., 4 H, *p*-CH Ph), 6.86 (br., 8 H, *m*-CH Ph), 7.41 (br *pseudo*-t, 8 H, *o*-CH Ph) ppm. ^{13}C NMR: δ = 43.3 (s, 2C, CH$_3$), 46.1 (s, 4C, CH$_3$), 57.3 (s, 4C, CH$_2$), 58.8 (s, 2C, CH$_2$), 121.0 (br., 4C, *p*-CH Ph), 127.7 (d, $^3J_{PC}$ = 5.2 Hz, 8C, *m*-CH Ph), 131.2 (m, 8C, *o*-CH Ph), 153.1 (d, $^1J_{PC}$ = 32.9 Hz, 4C, *i*-C Ph) ppm. ^{31}P{^{1}H} NMR: δ = –13.0 (s) ppm. The NMR spectroscopic data indicate complete substitution of hmteta by [D$_8$]THF in solution.

Crystal Structure Determinations: The intensity data for the compounds was collected on a Nonius KappaCCD diffractometer

Table 2. Crystal data and refinement details for the X-ray structure determinations of **1**, **2a**, **2b**, **3**, and **4**.

Compound	*cis*-**1**	**2a**	**2b**	**3**	**4**
Formula	C$_{40}$H$_{52}$CaO$_4$P$_2$·2C$_4$H$_8$O	C$_{40}$H$_{44}$CaN$_8$P$_2$	C$_{40}$H$_{44}$N$_8$P$_2$Sr	C$_{36}$H$_{50}$CaN$_4$P$_2$	C$_{36}$H$_{50}$CaN$_4$OP$_2$·1.5C$_7$H$_8$
fw /g mol^{-1}	843.04	738.85	786.39	640.82	795.02
T /°C	–140(2)	–90(2)	–90(2)	–140(2)	–140(2)
Crystal system	monoclinic	monoclinic	monoclinic	monoclinic	monoclinic
Space group	*C*2/*c*	*P*2$_1$/*n*	*P*2$_1$/*n*	*C*2/*c*	*C*2/*c*
a /Å	28.3842(4)	9.8382(8)	10.0306(3)	17.4513(7)	42.9287(10)
b /Å	8.4877(1)	17.967(2)	17.5212(9)	11.2393(7)	11.6140(4)
c /Å	22.0814(3)	10.9869(13)	11.2950(5)	17.8468(7)	17.9756(7)
β /°	120.508(1)	95.765(7)	95.213(3)	92.367(3)	97.159(2)
V /Å^3	4583.29(10)	1932.3(4)	1976.86(15)	3497.5(3)	8892.3(5)
Z	4	2	2	4	8
ρ /g cm^{-3}	1.222	1.270	1.321	1.217	1.188
μ /mm^{-1}	2.53	2.85	14.84	3.01	2.51
Measured data	14022	11885	13269	9988	22387
Data with $I > 2\sigma(I)$	4608	2913	2917	2770	7250
Unique data (R_{int})	5232/0.0233	4378/0.0968	4485/0.0583	3918/0.0576	9610/0.0535
wR_2 (all data, on F^2)[a]	0.1129	0.1810	0.1144	0.1739	0.2538
R_1 [$I > 2\sigma(I)$][a]	0.0408	0.0671	0.0440	0.0722	0.0988
S [b]	1.009	0.977	0.940	1.116	1.126
Residual dens. /e Å^{-3}	0.956/–0.749	0.274/–0.409	0.316/–0.303	0.400/–0.462	0.822/–0.570
Absorption method	none	none	none	none	none

[a] Definition of the *R* indices: $R_1 = (\Sigma||F_o| - |F_c||)/\Sigma|F_o|$; $wR_2 = \{\Sigma[w(F_o^2 - F_c^2)^2]/\Sigma[w(F_o^2)^2]\}^{1/2}$ with $w^{-1} = \sigma^2(F_o^2) + (aP)^2$. [b] $s = \{\Sigma[w(F_o^2 - F_c^2)^2]/(N_o - N_p)\}^{1/2}$.

using graphite-monochromated Mo-K_α radiation. Data was corrected for Lorentz and polarization effects but not for absorption effects.[28,29] The structures were solved by direct methods (SHELXS[30]) and refined by full-matrix least-squares techniques against F_o^2 (SHELXL-97[30]). A disorder has been observed in the hmteta ligand of **3**, with three carbon and two nitrogen atoms in two possible positions with refined occupancy factors of 0.5 and 0.5. All hydrogen atoms for *cis*-**1** and for both phenyl-groups of **3** were located by difference Fourier synthesis and refined isotropically. All other hydrogen atoms were included at calculated positions with fixed thermal parameters. All non-hydrogen atoms were refined anisotropically.[30] Crystallographic data as well as structure solution and refinement details are summarized in Table 2. XP (SIEMENS Analytical X-ray Instruments, Inc.) was used for structure representations.

CCDC-815843 (for **1**), -815844 (for **2a**), -815845 (for **2b**), -815846 (for **3**), and -815847 (for **4**) contain the supplementary crystallographic data for this paper. These data can be obtained free of charge from The Cambridge Crystallographic Data Centre via www.ccdc.cam.ac.uk/data_request/cif.

Acknowledgments

We thank the Deutsche Forschungsgemeinschaft (DFG) for generous financial support of this research initiative. F. Y. is grateful to the Deutscher Akademischer Austausch Dienst, (DAAD for a student exchange grant in the framework of International Association for the Exchange of Students for Technical Experience (IAESTE).

[1] a) M. Westerhausen, *Trends Organomet. Chem.* **1997**, *2*, 89–105; b) M. Westerhausen, *Coord. Chem. Rev.* **1998**, *176*, 157–210; c) M. Westerhausen, *Z. Anorg. Allg. Chem.* **2009**, *635*, 13–32.

[2] M. J. Harvey, T. P. Hanusa, *Organometallics* **2000**, *19*, 1556–1566.

[3] K. F. Tesh, D. J. Burkey, T. P. Hanusa, *J. Am. Chem. Soc.* **1994**, *116*, 2409–2417.

[4] M. Gärtner, H. Görls, M. Westerhausen, *Z. Anorg. Allg. Chem.* **2007**, *633*, 2025–2031.

[5] M. R. Crimmin, A. G. M. Barrett, M. S. Hill, P. B. Hitchcock, P. A. Procopiou, *Inorg. Chem.* **2007**, *46*, 10410–10415.

[6] a) T. M. A. Al-Shboul, H. Görls, M. Westerhausen, *Inorg. Chem. Commun.* **2008**, *11*, 1419–1421; b) T. M. A. Al-Shboul, V. K. Pálfi, L. Yu, R. Kretschmer, K. Wimmer, R. Fischer, H. Görls, M. Reiher, M. Westerhausen, *J. Organomet. Chem.* **2011**, *696*, 216–227.

[7] For excellent reviews on calcium-based catalysis, see: a) S. Harder, *Chem. Rev.* **2010**, *110*, 3852–3876; b) A. G. M. Barrett, M. R. Crimmin, M. S. Hill, P. A. Procopiou, *Proc. R. Soc. London Ser. A* **2010**, *466*, 927–963.

[8] M. R. Crimmin, A. G. M. Barrett, M. S. Hill, P. B. Hitchcock, P. A. Procopiou, *Organometallics* **2007**, *26*, 2953–2956.

[9] G. Mösges, F. Hampel, M. Kaupp, P. v. R. Schleyer, *J. Am. Chem. Soc.* **1992**, *114*, 10880–10889.

[10] M. Westerhausen, R. Löw, W. Schwarz, *J. Organomet. Chem.* **1996**, *513*, 213–229.

[11] M. Westerhausen, W. Schwarz, *Z. Anorg. Allg. Chem.* **1996**, *622*, 903–913.

[12] M. Westerhausen, W. Schwarz, *J. Organomet. Chem.* **1993**, *463*, 51–63.

[13] M. Kaupp, P. v. R. Schleyer, *J. Am. Chem. Soc.* **1992**, *114*, 491–497.

[14] R. J. Gillespie, S. Noury, J. Pilmé, B. Silvi, *Inorg. Chem.* **2004**, *43*, 3248–3256. For a detailed discussion of non-VSEPR structures of d^0-systems, see: M. Kaupp, *Angew. Chem.* **2001**, *113*, 3642; *Angew. Chem. Int. Ed.* **2001**, *40*, 3534–3565.

[15] M. Hargittai, *Chem. Rev.* **2000**, *100*, 2233–2301.

[16] S. Aldridge, A. J. Downs, *Chem. Rev.* **2001**, *101*, 3305–3365.

[17] J. Langer, S. Krieck, R. Fischer, H. Görls, M. Westerhausen, *Z. Anorg. Allg. Chem.* **2010**, *636*, 1190–1198.

[18] M. Gärtner, R. Fischer, J. Langer, H. Görls, D. Walther, M. Westerhausen, *Inorg. Chem.* **2007**, *46*, 5118–5124.

[19] G. W. Rabe, G. P. A. Yap, A. L. Rheingold, *Inorg. Chem.* **1995**, *34*, 4521–4522.

[20] G. W. Rabe, J. Riede, A. Schier, *Main Group Chem.* **1996**, *1*, 273–277.

[21] G. W. Rabe, G. P. A. Yap, A. L. Rheingold, *Inorg. Chim. Acta* **1998**, *262*, 309–311.

[22] S. Blair, K. Izod, W. Clegg, *Inorg. Chem.* **2002**, *41*, 3886–3893.

[23] S. Blair, K. Izod, W. Clegg, R. W. Harrington, *Inorg. Chem.* **2004**, *43*, 8526–8531.

[24] H. H. Karsch, M. Reisky, *Eur. J. Inorg. Chem.* **1998**, 905–911.

[25] M. Gärtner, H. Görls, M. Westerhausen, *Organometallics* **2007**, *26*, 1077–1083.

[26] M. S. Hill, M. F. Mahon, T. P. Robinson, *Chem. Commun.* **2010**, *46*, 2498–2500.

[27] See for instance the following reviews: a) R. C. Mehrotra, A. Singh, S. Sogani, *Chem. Soc. Rev.* **1994**, *23*, 215–225; b) K. M. Fromm, E. D. Gueneau, *Polyhedron* **2004**, *23*, 1479–1504; c) K. M. Fromm, *Dalton Trans.* **2006**, 5103–5112.

[28] *COLLECT*, Data Collection Software, Nonius B. V., The Netherlands, **1998**.

[29] Z. Otwinowski, W. Minor, in: *Methods in Enzymology*, vol. 276, *Macromolecular Crystallography*, part A: *Processing of X-ray Diffraction Data Collected in Oscillation Mode* (Eds.: C. W. Carter, R. M. Sweet), Academic Press, **1997**, pp. 307–326.

[30] G. M. Sheldrick, *Acta Crystallogr., Sect. A* **2008**, *64*, 112–122.

Received: March 9, 2011
Published Online: May 24, 2011

